

# Electric Field-Induced Oxidation of Ferromagnetic/ Ferroelectric Interfaces

Sebastien Couet,\* Manisha Bisht,\* Maarten Trekels, Mariela Menghini, Claire Petermann, Margriet J. Van Bael, Jean-Pierre Locquet, Rudolf Ruffer, André Vantomme, and Kristiaan Temst

Composite multiferroics are a new class of material where magneto-electric coupling is achieved by creating an interface between a ferromagnetic and a ferroelectric compound. The challenge of understanding the chemical and magnetic properties of such interface is a key to achieve good magneto-electric coupling. The unique possibilities offered by isotope sensitive techniques are used to selectively investigate the interface's chemistry and magnetism in Fe/BaTiO<sub>3</sub> and Fe/LiNbO<sub>3</sub> systems during the application of an electric field. With a large enough electric field, a strong oxidation of Fe is triggered, which creates a magnetically dead interface. This leads to an irreversible decrease of the magneto-electric coupling properties. Material parameters are identified that determine under which electric field the interface may be modified. The results are confirmed on the two systems and are expected to be widespread in this new class of hybrid material.

## 1. Introduction

Metal/ferroelectric interfaces are found in many systems such as contacts on piezoelectric transducers and capacitors. Recently, such heterostructures became increasingly important in the field of multiferroics, a class of material that combines at least two ferroic properties such as ferroelectricity and ferromagnetism.<sup>[1,2]</sup> Since bulk multiferroic materials are rare,<sup>[3]</sup> another approach has been developed whereby multiferroic properties are artificially induced by combining a ferromagnetic (FM) and a ferroelectric (FE) coupled through an interface.<sup>[1,4-6]</sup> In these materials, the aim is to control the magnetic properties of the system (magnetization direction, domain state, etc.) using electric fields. The magneto-electric coupling

can be achieved for example through the intrinsic properties of the materials like magnetostriction and piezoelectric effect. Application of an electric field on the ferroelectric will induce a strain which can be transferred to the adjacent ferromagnetic layer and change its magnetic properties. A variety of experiments on these heterostructures have been recently reported. Magnetization switching has been demonstrated in bonded ferromagnetic/ferroelectric bilayers.<sup>[6]</sup> Electric field controlled superparamagnetic/ferromagnetic transition has been observed in Nickel/Piezoelectric composites.<sup>[7]</sup> More directly related to interfacial effects, correlation between stress states and magnetic domains has been observed in a Ni/BaTiO<sub>3</sub> system.<sup>[8]</sup>

The change of coercivity induced by the application of an electric field in FM/FE bilayers has already been reported for a number of systems.<sup>[9-11]</sup>

The interfacial structure and chemistry in these systems are two crucial aspects of their functionality since they determine the magneto-electric (ME) coupling. Ferroelectric materials often incorporate oxygen. The interface with a metal can thus be rather complex since oxidation of the metal is likely to take place.<sup>[12-14]</sup> The resulting transition metal oxide layer formed at the interface may show a different stoichiometry, thickness, structure and magnetic state depending on the constituting elements.<sup>[12]</sup> The Fe/BaTiO<sub>3</sub> interface is a good model system for ME coupling. On one hand, it has been reported that deposition of Fe on BaTiO<sub>3</sub>(BTO) leads to the formation of an interfacial iron oxide layer (primarily Fe<sup>2+</sup>).<sup>[13,14]</sup> On the other hand, deposition of BTO on Fe films can produce an iron oxide-free interface.<sup>[15]</sup> Taking it one step further, the effect of the applied electric field itself on the chemical and magnetic state of the interface remains unclear in such metal/ferroelectric systems.

Obtaining direct information on both the chemical and magnetic state of such buried interface during the application of an electric field is a real challenge. Most structural characterization techniques either rely on partial sample destruction (transmission electron microscopy) or are not sensitive enough to extract interfacial information. Element specific methods like X-ray magnetic dichroism can be used, but they will typically integrate the signal over the full FM film for example. In that respect, nuclear techniques based on isotopic sensor layers

Dr. S. Couet, M. Bisht, M. Trekels, C. Petermann,  
Prof. A. Vantomme, Prof. K. Temst  
Instituut voor Kern-en Stralingsfysica  
KU Leuven, Celestijnenlaan 200D, B-3001, Leuven, Belgium  
E-mail: Sebastien.couet@fys.kuleuven.be;  
Manisha.bisht@fys.kuleuven.be

Dr. M. Menghini, Prof. M. J. Van Bael, Prof. J.-P. Locquet  
Laboratorium voor Vaste-Stoffysica en Magnetisme  
KU Leuven, Celestijnenlaan 200D, B-3001, Leuven, Belgium  
Dr. R. Ruffer

European Synchrotron Radiation Facility (ESRF)  
BP 220, F-38043, Grenoble, Cedex, France



DOI: 10.1002/adfm.201301160

like Mössbauer spectroscopy, which are sensitive only to specific isotopes like  $^{57}\text{Fe}$  (and not  $^{56}\text{Fe}$ ) offers the possibility to constrain the recorded signal to the few atomic layers of the interface. The synchrotron-based variant, nuclear resonant scattering, even allows more complex conditions to be used,<sup>[16]</sup> like the simultaneous application of an electric field.

In this article, we present a study of the chemistry and local magnetic properties of the interface region both as-grown and under applied electric field in two model systems of FM/FE compound:  $\text{Fe}/\text{BaTiO}_3$  and  $\text{Fe}/\text{LiNbO}_3$ . To gain high sensitivity and site selectivity to the interface, we used the isotope sensitive techniques of Mössbauer spectroscopy (MS) and nuclear resonant scattering (NRS) of synchrotron radiation. This enables to use an *isotopic probe layer* scheme where a selected part of the Fe film is enriched with  $^{57}\text{Fe}$ .<sup>[16]</sup> The recorded signal is limited to the position in the sample where the  $^{57}\text{Fe}$  layer is deposited. NRS specifically allows to follow the evolution of the interface's chemical and magnetic nature while applying an electric field. The observed structural changes are analyzed in the framework of electric field induced ion transport at metal-oxide interfaces. This highlights the determining roles of the work function difference between the two materials and the dielectric constant of the ferroelectric. The present findings have direct implications for the broad field of metal/ferroelectric systems where electric fields are applied to polarize the ferroelectric, as well as for the emerging field of composite multiferroics materials. Our results add a better understanding of the reactions occurring at metal/oxide interfaces in general.

## 2. Results and Discussion

First, we study how the chemistry and magnetism of a FM/FE interface evolves upon applying an electric field on the Fe/BTO system. The interface sensitivity is achieved by isotopic doping of the interface with  $^{57}\text{Fe}$ , which is the active isotope for MS and NRS here. The sample structure we used consists of  $\text{BTO}(100)/^{57}\text{Fe}(1\text{ nm})/^{56}\text{Fe}(2\text{ nm})/^{57}\text{Fe}(0.5\text{ nm})/^{56}\text{Fe}(1.5\text{ nm})/\text{Al}(5\text{ nm})$ , as shown in **Figure 1**. More details on the sample growth are found in the Experimental section. Since NRS is only sensitive to the  $^{57}\text{Fe}$  isotope (i.e. not to  $^{56}\text{Fe}$ ), the signal collected in the experiment originates only from the two  $^{57}\text{Fe}$  probe layers which will be referred to as interface layer and middle layer respectively since they provide information about those parts of the Fe film. In NRS, the hyperfine parameters

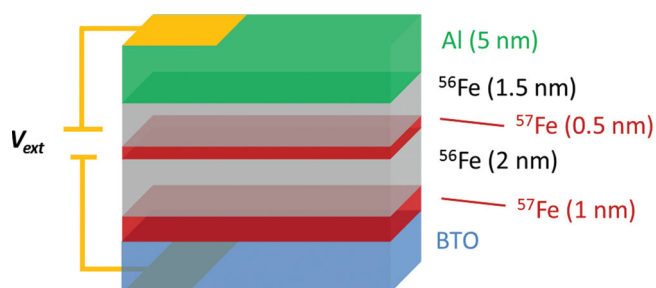


**Figure 1.** Schematic view of the sample structure used in the NRS experiment. The recorded signal originates from the two  $^{57}\text{Fe}$  probe layers.

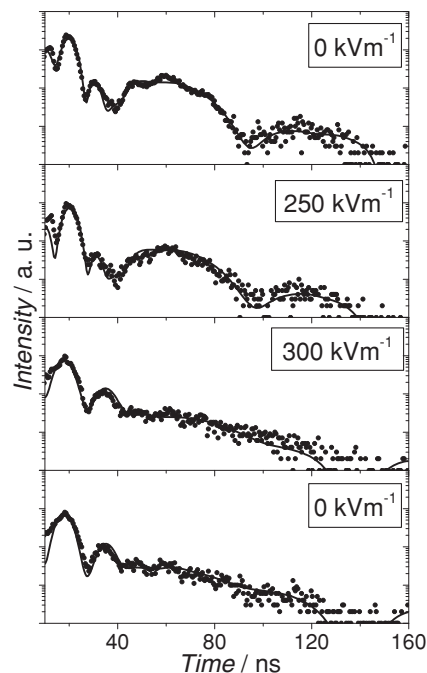


**Figure 2.** Nuclear time spectra of the  $\text{BTO}/^{57}\text{Fe}(1\text{ nm})/^{56}\text{Fe}(2\text{ nm})/^{57}\text{Fe}(0.5\text{ nm})/^{56}\text{Fe}(1.5\text{ nm})$  system upon application of an electric field. The solid lines are fits to the data. An irreversible change of structure appears at  $300\text{ kV m}^{-1}$ .

of the Mössbauer isotope are obtained by measuring the time dependent de-excitation of the  $^{57}\text{Fe}$  nuclei after pulsed excitation with synchrotron radiation.<sup>[17]</sup> From the obtained hyperfine parameters, one can deduce the chemical and magnetic state of the  $^{57}\text{Fe}$  atoms at the interface via the isomer shift and the hyperfine magnetic field.<sup>[17–19]</sup> NRS does not only combine the isotope sensitivity of Mössbauer spectroscopy with the fast acquisition time achievable at third generation synchrotron sources: it enables depth sensitivity via the grazing incidence x-ray scattering geometry which is used here. Although the recorded time spectra include signals from both  $^{57}\text{Fe}$  layers, x-ray interference effects in grazing incidence allow to disentangle the contributions of each layer to the signal in the fitting procedure.<sup>[19]</sup>

Consecutive nuclear time spectra have been recorded at increasing positive voltage with  $25\text{ kV m}^{-1}$  steps applied on the sample (by convention, positive voltage means positive potential is applied on the Fe film side). From 0 to  $250\text{ kV m}^{-1}$  (above the coercive field of BTO which is around  $100\text{ kV m}^{-1}$ ),<sup>[20]</sup> almost no changes are observed in the time spectra, as shown in **Figure 2** (only a subset of the recorded timespectra are plotted). At a threshold electric field of  $300\text{ kV m}^{-1}$ , a drastic change appears which is irreversible since the spectrum does not recover when returning to a field of  $0\text{ kV m}^{-1}$ . The hyperfine parameters listed in **Table 1** were obtained from fitting the timespectra: the isomer shift *IS* which mainly depends on the oxidation state of the  $^{57}\text{Fe}$  atom, the quadrupole splitting *QS* related to the site symmetry and the hyperfine field magnitude  $B_{\text{hf}}$  which is proportional to the atomic magnetic moment.

As can be expected, the middle layer is composed of pure ferromagnetic Fe, however, with  $B_{\text{hf}} = 26.9\text{ T}$  slightly lower

**Table 1.** Parameters extracted from the time spectra recorded at 250 kV<sup>m</sup><sup>-1</sup> (i.e. the same as for the as-grown state) and 300 kV<sup>m</sup><sup>-1</sup> (i.e. the same as the “reset to zero” state). The top part corresponds to the middle layer represented by one state while the interface layer (lower part) is modeled by three states. The main parameter changes at 300 kV<sup>m</sup><sup>-1</sup> are bold.

Layer	State	Isomer shift [mm/s]		Quad. Splitting [mm/s]		Hyperfine field [T]		Weight [%]	
		250 kV <sup>m</sup> <sup>-1</sup>	300 kV <sup>m</sup> <sup>-1</sup>	250 kV <sup>m</sup> <sup>-1</sup>	300 kV <sup>m</sup> <sup>-1</sup>	250 kV <sup>m</sup> <sup>-1</sup>	300 kV <sup>m</sup> <sup>-1</sup>	250 kV <sup>m</sup> <sup>-1</sup>	300 kV <sup>m</sup> <sup>-1</sup>
Middle	1 (metal)	0	0	0	0	26.9	29.2	100	100
	1 (metal)	0.55	0.71	0	0	27	29.2	36	<b>16</b>
Interface	2 (oxide)	0.75	–	0.082	–	42	–	47	<b>0</b>
	3 (oxide)	0.92	<b>0.50</b>	0.15	0.18	0	0	17	<b>84</b>

than the well-established bulk value of 33.3 T. This decrease is attributed to the proximity to the interface. The interface layer itself is modeled using three different configurations. Only 36% of the layer shows properties of ferromagnetic Fe (state 1 in Table 1). Since 1 nm of <sup>57</sup>Fe has initially been deposited, this means that as much as 0.65 nm of Fe oxidizes when deposited onto the BTO substrate. This oxidized layer is a mixture of both a magnetic (state 2) and a non-magnetic (state 3) component. The fit indicates that the magnetic component has the largest weight and exhibit an IS and B<sub>hf</sub> close to what has been reported for magnetic Fe<sup>2+</sup> sites in ultrathin iron oxide layers.<sup>[21]</sup> The results for the 300 kV<sup>m</sup><sup>-1</sup> and “reset to 0 kV<sup>m</sup><sup>-1</sup>” spectra show that the composition of the interface layer has changed after applying a positive electric field. The magnetic oxide component completely disappears and only a single non-magnetic site with a lower IS of 0.5 mm/s remains. This IS indicates that an oxygen-rich Fe<sup>3+</sup> oxide has formed.<sup>[22]</sup> The electric polarization process also leads to further oxidization of the Fe metal, such that in the end as much as 0.85 nm of Fe has oxidized. Assuming an average volume growth factor between 1.5 and 2.4 for an iron oxide phase compared to pure Fe,<sup>[23]</sup> the result at 300 kV<sup>m</sup><sup>-1</sup> corresponds to an interface layer which is 1.2 to

2 nm thick. In summary, a thicker, oxygen-rich and non-magnetic interface oxide layer has been formed after applying an electric field of 300 kV<sup>m</sup><sup>-1</sup>.

These results raise the question what is the role of the electric field in modifying the interface structure. In general, oxidation/reduction reactions take place when a reactive metal is deposited on an oxide surface due to a mismatch of the work functions of the two materials.<sup>[24]</sup> Since the Fermi levels in the two material have to be connected, the difference in work function (typically below 1 V) induces a large interfacial electric field which promotes the diffusion of metal and/or oxygen ions, as shown in **Figure 3**. In the case of the Fe/BTO system, the work function difference  $V_i = \phi_{Fe} - \phi_{BTO}$  is approximately 0.5 V, assuming bulk values.<sup>[25]</sup> The large electric field E<sub>0</sub> induced by the presence of V<sub>i</sub> at the interface promotes the diffusion of ions, in turns leading to the creation of an interface oxide layer as well as a narrow charged region around it, as shown in Figure 3. This is the actual situation after thin film growth and is the result of simple electrostatic effects. The application of an external voltage V<sub>ext</sub> in modifying the interface structure can be understood in the same framework. The critical point is to estimate the additional voltage drop V<sub>A</sub> induced at the interface by V<sub>ext</sub>. One way to calculate V<sub>A</sub> is to treat the substrate/interface system as two capacitors placed in series, each with its own permittivity, and then subsequently expressing the voltage drop across one of the two capacitors (the interface):

$$V_A = \frac{Q}{C_{int}} = \frac{C_{tot}}{C_{int}} V_{ext} \quad (1)$$

where C<sub>int</sub> and C<sub>tot</sub> are the interface and total capacity, respectively. Since in our case C<sub>BTO</sub> << C<sub>int</sub> because of the large thickness of the substrate, C<sub>tot</sub> ≈ C<sub>BTO</sub>.

$$V_A \approx \frac{C_{BTO}}{C_{int}} V = \frac{\epsilon_{BTO}}{\epsilon_{int}} \frac{d_{int}}{d_{BTO}} V_{ext} \quad (2)$$

d<sub>int</sub> is the thickness of the interface oxide which has been estimated to be around 1.6 nm. If we assume a relative permittivity ε<sub>BTO</sub> = 2000 for BTO at room temperature and ε<sub>int</sub> = 15 for the interface oxide (value for an Fe<sup>3+</sup> iron oxide phase),<sup>[26,27]</sup> V<sub>A</sub> has an approximate value of 0.13 V for V<sub>ext</sub> = 300 V.

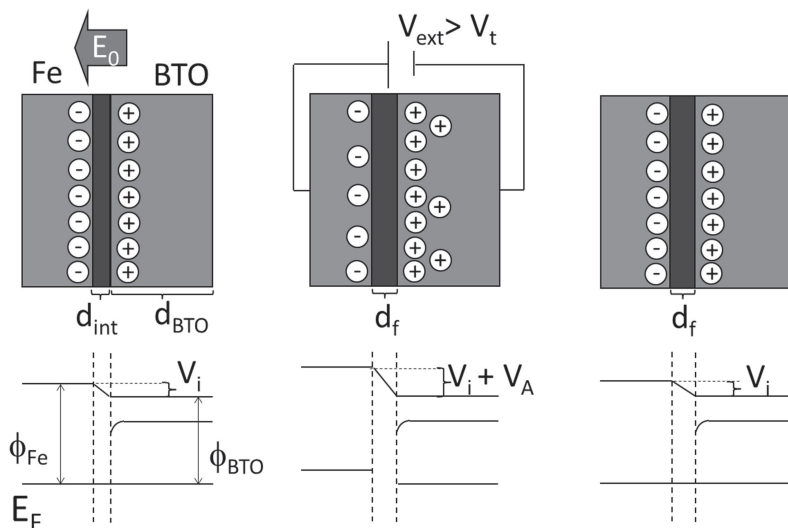


**Figure 3.** Static charge distribution (top) and electron potential energy diagram (bottom) at the Fe/BTO interface (from left to right) before, during and after application of a threshold voltage V<sub>t</sub>. V<sub>i</sub> is the interface potential induced by the work function difference V<sub>i</sub> = φ<sub>Fe</sub> – φ<sub>BTO</sub>. V<sub>A</sub> is the potential induced by the additional charges present once a voltage V<sub>ext</sub> is applied.

This induces an electric field  $E_A \approx 10^8 \text{Vm}^{-1}$  which is sufficient to trigger further ion transport across the interface.<sup>[24]</sup> Rewriting the equation in terms of electric fields, which are independent of the thicknesses of both the interface layer and the substrate gives:

$$E_A = \frac{\epsilon_{\text{BTO}}}{\epsilon_{\text{int}}} E_{\text{ext}} \quad (3)$$

The equation shows that  $\epsilon_{\text{BTO}}$  is the main variable parameter (apart of  $E_{\text{ext}}$  of course) for the appearance of a large interface field. Indeed, one of the particular features of a ferroelectric material such as BTO is its large permittivity. If BTO would be replaced by a conventional oxide with  $\epsilon \approx 15$  there would be virtually no additional electric field across the interface upon application of  $V_{\text{ext}}$ . It should be noted that the initial surface structure of BTO can modify the workfunction.<sup>[25]</sup> This means that surface defects or reconstructions can modify the initial interface voltage  $V_i$ .

The presented electric field induced ion diffusion does not at first sight involve a voltage threshold mechanism as we have observed from the NRS measurements. However, it is well known that in the low temperature high electric field case the ionic diffusion current  $J$  at a metal/oxide interface shows an exponential dependence on the electric field:<sup>[24]</sup>

$$J \approx \sinh(Ze E_A a / k_B T) \quad (4)$$

where  $Z$  is the charge number,  $e$  the elementary charge,  $a$  the lattice parameter and  $T$  the temperature. We calculate that for the estimated values of  $V_A$  and  $E_A$  near threshold, an increase in  $V_{\text{ext}}$  of 50 V (which is the experimental stepsize) leads to an increase of  $J$  by more than two orders of magnitude. This exponential dependence may thus well produce a voltage threshold effect as observed in our experiment. It will be worth in the future to study in more detail the possible occurrence of the observed interface oxidation over longer time at lower voltages since it could eventually be detrimental for the long term use of devices. In this perspective, it should be noted that the present findings are only examined in DC mode, i.e., the time and cycle dependence of the interface properties and magneto-electric coupling has not been investigated. It has recently been shown that aging effects were taking place in FM/FE heterostructures either due to ferroelectric, magnetic or stress relaxation.<sup>[29]</sup> The modification of the interface structure evidenced here may yet be another contributor for aging effects in FM/FE composites.

Summarizing, the presented model shows that the main parameters determining the occurrence of electric field induced oxidation are  $V_i$ , the work function difference between the two materials, and  $\epsilon$ , the dielectric constant of the ferroelectric. According to this model, the process is not symmetric: depending on the value of  $V_i$  and the sign of the applied electric field,  $V_A$  either adds to or subtracts from  $V_i$ . The evolution of the system upon application of an electric field will then depend on the strength of  $V_i$  compared to  $V_A$ . For  $V_A < V_i$ , diffusion may occur only when  $V_A$  and  $V_i$  adds up while for  $V_A > V_i$ , diffusion may appear for both voltage polarity. We performed Mössbauer spectroscopy experiments to study the dependence on the sign of the applied voltage in the Fe/BTO system. Fe/LiNbO<sub>3</sub> (LNO) was also investigated, since it presents a lower  $\epsilon$  and hence

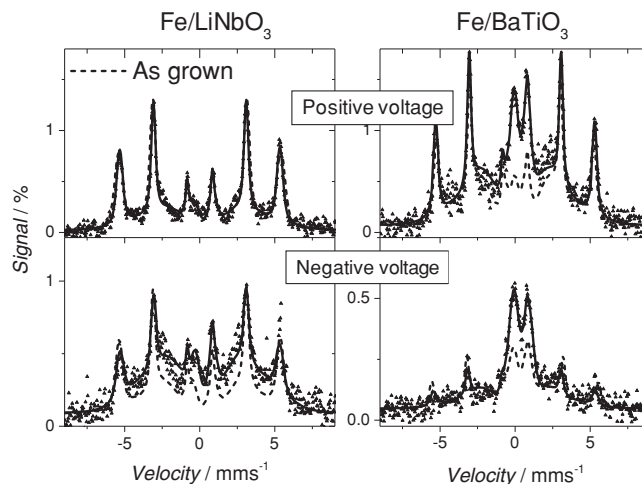


**Figure 4.** Mössbauer spectroscopy measurements on LNO and BTO substrates with the following layer sequence: substrate/<sup>57</sup>Fe(0.5 nm)/<sup>56</sup>Fe(4.5 nm)/Al(5 nm). The spectra have been recorded for samples as-grown and after application of a positive and a negative field. The dashed lines are the fits of the as grown spectra. All measurements are done in a zero electric field. Structural changes appear for negative field only for Fe/LNO and positive as well as negative field for Fe/BTO.

potentially a lower  $V_A/V_i$  ratio. It also shows a negative  $V_i$ , and should consequently behave in the opposite way compared to the Fe/BTO system, i.e. negative  $V_{\text{ext}}$  should induce diffusion. Indeed LNO has a work function that varies from 4.6 to 6.2 V in case the surface is positively or negatively poled, respectively.<sup>[28]</sup> In our study, we used unpoled substrates that should have an average work function of 5.4 eV, in any case larger than for Fe. In these experiments, only a single 1 nm <sup>57</sup>Fe probe layer was deposited at the interface, the remaining 4 nm being <sup>56</sup>Fe, such that only the interface is probed. Mössbauer spectra were recorded for three cases: as grown, after application of +600 kVm<sup>-1</sup> and after -600 kVm<sup>-1</sup> (each time on a new, fresh sample). The measurements are all carried out in zero electric field. The results for both the Fe/LNO and Fe/BTO systems are shown in **Figure 4**. In each case, the as-grown spectrum is shown as dashed line. For Fe/LNO, a negative voltage leads to a change in the interface structure, with an increase of the non-magnetic fraction. A positive voltage does not modify the interface. These observations are consistent with our model, since in the case of negative  $V_i$  ion diffusion will be occurring faster with a negative external field. The fact that nothing happens for positive values is consistent with  $V_A < V_i$ . For Fe/BTO, we observe the same phenomenon as in the NRS experiment: a modification of the interface structure upon application of a positive electric field. However, a negative field does also modify the interface. The very high  $\epsilon_{\text{BTO}}$  and the high field applied here (600 kVm<sup>-1</sup>) leads to a sufficiently large  $V_A$  value to promote an ionic diffusion even with negative polarity. These results show that the observed electric field induced oxidation is likely to take place in many metal/ferroelectric systems presenting a large permittivity of the dielectric. It should be noted that in each cases the proportion of oxidized non-magnetic states (represented by the central doublet peak structure in the Mössbauer spectra) is increasing after electric polarization. This means that



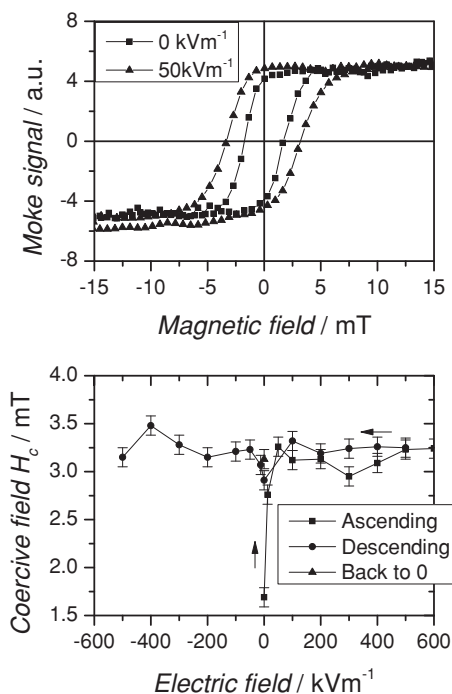


**Figure 5.** Top panel: Room temperature magnetic hysteresis curve recorded on a BTO/Fe(5 nm)/Al(5 nm) sample at 0 and 50 kV $m^{-1}$ . The bottom panel shows the evolution of the coercive field  $H_c$  as a function of electric field.  $H_c$  never returns to its initial value, even with negative polarity cycling.

in all the studied cases it results in the formation of a magnetically dead interface layer. This finding is a key point for controlling the interface structure in multiferroic composite materials.

It should be noted that these electric field induced diffusion phenomenon are in principle accompanied by a part of irreversibility. Indeed once ion diffusion has taken place, the interface thickness has increased, which means that the overall electric field present across the interface (for a given  $V_{ext}$ ) will decrease. It should also be noted that, according to the interface ionic diffusion processes discussed by Fu et al.,<sup>[24]</sup> the sign of the electric field typically determines the moving species (oxygen or metal atoms) but in both cases this movement contributes at increasing the interface thickness. As such, applying an opposite polarity after the interface has been modified can hardly restore the exact initial stage but will rather create a new intermediate stage again. This kind of aging process should be studied in more detail in the future.

The formation of a magnetically dead interface layer has significant implications for the magneto-electric properties of multiferroic composites. We measured magnetic hysteresis curves on a pristine Fe/BTO (with exactly the same layer structure as used in the NRS experiment) and when applying a positive electric field. As shown in **Figure 5**, the magnetic coercive field  $H_c$  increases by more than 90% upon application of an electric field up to the ferroelectric coercive field of BTO. This is presumably due to a magneto-electric coupling effect induced by switching of the ferroelectric domains. However,  $H_c$  does not recover to its original value when cycling back to 0 kV $m^{-1}$  or even applying

negative polarity, an effect which was also reported by Sahoo et al.<sup>[10]</sup> Measurements on different samples show that the percentage increase in coercivity may vary. Since samples are grown in the same conditions, we expect that the initial BTO surfaces play an important role for an efficient coupling. According to the results presented here, we believe that the non-return to the original  $H_c$  is due to the permanent structural change of the interface (which leads to a permanent change of the magnetic anisotropy) induced by  $E_{ext}$ . The magnetically dead oxide layer effectively reduces the ME coupling (reduction of the change in  $H_c$ ). It acts as a decoupling spacer layer. In order to improve the ME coupling, one thus needs to control the electric field induced diffusion at the interface so as to minimize the thickness of the interface oxide. Two parameters should be taken into account: the work function difference of the two materials should be as small as possible while a lower relative permittivity of the ferroelectric will decrease the induced electric field  $E_A$ . The design of new ferromagnetic-ferroelectric composites should take these phenomena into account.

### 3. Conclusions

We have shown that an irreversible oxidation/reduction process can be induced at an Fe/ferroelectric interface by applying an electric field. These observations have been made possible by isolating the signal from the buried interface using isotopic sensor layers. This behavior has been observed in two systems, indicating it will probably happen for a wide selection of ferromagnetic and ferroelectric materials. This process eventually leads to the formation of a magnetically dead interface layer which reduces the magneto-electric coupling properties of the system. The mechanism at the basis of the extra interdiffusion is understood as the induction of an additional electric field  $E_A$  across the interface.  $E_A$  is mainly influenced by the large permittivity of ferroelectric materials which is a key parameter of this electric field induced interdiffusion. In order to use the magneto-electric coupling, one has to understand and control the chemical and physical changes that can occur at the interface. Material's parameters such as the work function difference and the dielectric constant of the ferroelectric are crucial in determining the oxidation behavior of the interface and should be taken into account in further designs. On the other hand, the modification of the interface structure upon application of an electric field could also be beneficial, depending on the system. The growth of a thicker oxide layer may in some cases trigger new interfacial coupling properties. For example, CoO is an antiferromagnet which could play an important role at a cobalt/ferroelectric interface by implementing in a unique way exchange biasing in the system.<sup>[30]</sup> The presented findings are thus not only important for understanding magneto-electric coupling in present day systems but can trigger new ways of preparing and controlling interface properties by means of an electric field.

### 4. Experimental Section

The samples have been grown by molecular beam epitaxy (MBE) at 50 °C on 0.5 mm thick polished BaTiO<sub>3</sub>(001) and LiNbO<sub>3</sub>(0001) single

crystals. The Fe layers have been deposited using two Knudsen cells with isotopically enriched  $^{57}\text{Fe}$  (>99.2%) and  $^{56}\text{Fe}$  (99.8%), respectively. The use of a  $^{56}\text{Fe}$  enriched source compared to a  $^{nat}\text{Fe}$  source allows to eliminate small contribution to the signal of the  $^{57}\text{Fe}$  present in natural Fe. We calculate in our case that more than 99.9% of the signal originates effectively from the  $^{57}\text{Fe}$  probe layers. Finally, the samples have been capped by 5 nm of Al to prevent surface oxidation. Macroscopic silver paint electrical contacts were made at the bottom and at the top of the substrate to apply an electric field across the thickness of the substrate. The NRS experiment was carried out at the ID22N Nuclear Resonance beamline of the ESRF (Grenoble, France).<sup>[31]</sup> The time spectra have been fitted using the CONUSS program package.<sup>[32]</sup>

## Acknowledgements

S. Couet and M. Bisht contributed equally to this work. S.C. thanks the Flemish Science Foundation (FWO-VI) for individual financial support. This work was supported by the Concerted Research Action programs (GOA/09/006) and (GOA/14/007).

Received: April 4, 2013

Revised: July 2, 2013

Published online: August 23, 2013

- [1] R. Ramesh, N. A. Spaldin, *Nature Mater.* **2007**, *6*, 22.
- [2] G. Catalan, J. F. Scott, *Adv. Mater.* **2009**, *21*, 2463.
- [3] M. Gajek, M. Bibes, S. Fusil, K. Bouzehouane, J. Fontcuberta, A. Barthélémy, A. Fert, *Nat. Mater.* **2007**, *6*, 296.
- [4] C. W. Nan, M. I. Bichurin, S. Dong, D. Viehland, G. Srinivasan, *J. Appl. Phys.* **2008**, *103*, 031101.
- [5] Y. Zhang, J. Liu, X. H. Xiao, T. C. Peng, C. Z. Jiang, H. H. Lin, C. W. Nan, *J. Phys. D: Appl. Phys.* **2010**, *43*, 082002.
- [6] Y. J. Chen, T. Fitchorov, C. Vittoria, V. G. Harris, *Appl. Phys. Lett.* **2010**, *97*, 052502.
- [7] H. K. D. Kim, L. T. Schelhas, S. Keller, J. L. Hockel, S. H. Tolbert, G. P. Carman, *Nano Lett.* **2013**, *13*, 884.
- [8] R. Streubel, D. Köhler, R. Schäfer, L. M. Eng, *Phys. Rev. B* **2013**, *87*, 054410.
- [9] C.-G. Duan, S. S. Jaswal, E. Y. Tsymlal, *Phys. Rev. Lett.* **2006**, *97*, 047201.
- [10] S. Sahoo, S. Polisetty, C.-G. Duan, S. S. Jaswal, E. Y. Tsymlal, C. Binek, *Phys. Rev. B* **2007**, *76*, 0921083.
- [11] G. Venkataiah, Y. Shirahata, M. Itoh, T. Taniyama, *Appl. Phys. Lett.* **2011**, *99*, 102506.
- [12] T. J. Regan, H. Ohldag, C. Stamm, F. Nolting, J. Lüning, J. Stöhr, R. L. White, *Phys. Rev. B* **2001**, *64*, 214422.
- [13] S. Brivio, C. Rinaldi, D. Petti, R. Bertacco, F. Sanchez, *Thin Solid Films* **2011**, *519*, 5804.
- [14] L. Bocher, A. Gloter, A. Crassous, V. Garcia, K. March, A. Zobelli, S. Valencia, S. Enouz-Vedrenne, X. Moya, N. D. Marthur, C. Deranlot, S. Fusil, K. Bouzehouane, M. Bibes, A. Barthélémy, C. Colliex, O. Stéphane, *Nano Lett.* **2012**, *12*, 376.
- [15] A. Zenkevich, R. Mantovan, M. Fanciulli, M. Minnekaev, Y. Matveyev, Y. Lebedinskii, S. Thiess, W. Drube, *Appl. Phys. Lett.* **2011**, *99*, 182905.
- [16] R. Röhlberger, H. Thomas, K. Schlage, E. Burkel, O. Leupold, R. Ruffer, *Phys. Rev. Lett.* **2002**, *89*, 237201.
- [17] R. Röhlberger, in *Springer Tracts in Modern Physics*, Vol. 208, Springer-Verlag, Berlin **2004**.
- [18] M. Slezak, T. Slezak, K. Freindl, W. Karas, N. Spiridis, M. Zajac, A. I. Chumakov, S. Stankov, R. Ruffer, J. Korecki, *Phys. Rev. B* **2013**, *87*, 134411.
- [19] S. Couet, Th. Diederich, S. Stankov, K. Schlage, T. Slezak, R. Ruffer, J. Korecki, R. Röhlberger, *Appl. Phys. Lett.* **2009**, *94*, 162501.
- [20] K. D. Schomann, *Appl. Phys.* **1975**, *6*, 89.
- [21] S. Couet, K. Schlage, S. Stankov, R. Ruffer, Th. Diederich, B. Laenens, R. Röhlberger, *Phys. Rev. Lett.* **2009**, *103*, 097201.
- [22] Mössbauer Spectroscopy Applied to Inorganic Chemistry, Vol.2 (Eds: G. J. Long, F. Grandjean), Plenum Press, New York **1987**.
- [23] G. S. D. Beach, F. T. Parker, D. J. Smith, P. A. Crozier, A. E. Berkowitz, *Phys. Rev. Lett.* **2003**, *91*, 267201.
- [24] Q. Fu, T. Wagner, *Surf. Sci. Rep.* **2007**, *62*, 431.
- [25] N. Barrett, J. Rault, I. Krug, B. Vilquin, G. Niu, B. Gautier, D. Albertini, P. Lecoeur, O. Renault, *Surf. Interface Anal.* **2010**, *42*, 1690.
- [26] G. Arlt, D. Henning, G. de With, *J. Appl. Phys.* **1985**, *58*, 1619.
- [27] <http://www.asiinstr.com/technical/Dielectric%20Constants.htm>, section D, accessed: March, 2013.
- [28] W.-C. Yang, B. J. Rodriguez, A. Gruverman, R. J. Nemanich, *Appl. Phys. Lett.* **2004**, *85*, 2316.
- [29] Y. Chen, A. L. Geiler, T. Fitchorov, C. Vittoria, V. G. Harris, *Appl. Phys. Lett.* **2009**, *95*, 182501.
- [30] S. Polisetty, W. Echtenkamp, K. Jones, X. He, S. Sahoo, C. Binek, *Phys. Rev. B* **2010**, *82*, 134419.
- [31] R. Ruffer, A. I. Chumakov, *Hyperfine Interact.* **1996**, *97/98*, 589.
- [32] W. Sturhahn, *Hyperfine interact.* **2000**, *125*, 149.